Original

Effect of Applied Parallel Electric Field on Electroosmotic Flow in Donut Channel

Tamio Fujiwara[1], Osami Kitoh[2] and Takao Tsuda[3]

Graduate School of Engineering, Nagoya Institute of Technology Gokiso, Showa, Nagoya 466-8555, Japan

Department of Mechanical Engineering, Nagoya Institute of Technology Gokiso, Showa, Nagoya 466-8555, Japan

Department of Applied Chemistry, Nagoya Institute of Technology Gokiso, Showa, Nagoya 466-8555, Japan

Received July 2, 2001. Revised manuscript received September 20, 2001. Accepted October 22, 2001.

Abstract

The influence of an electric field parallel to a silica-water interface on electroosmosis was studied by using a precisely manufactured apparatus. In this study, a donut channel constructed by a gap between two parallel donut-shaped glass plates was used for generating an electroosmotic flow of water. After adjusting the pressure gradient in the channel to zero, the electroosmotic flow rate was measured by an original micro-flow meter in the range of 0.1 to 2 [mm^3/sec]. It was shown that there were three different tendencies of the electroosmotic flow rate on the applied electric field. We supposed these differences were derived from the variation of the zeta potential with the electric field: decreasing, increasing and approaching constant. It was also shown that the variations in electroosmosis with the electric field had a relation to that of the electric current in the channel.

Keywords: Electroosmosis, Electroosmotic flow, Electric double layer, Zeta potential, Electric current

1 Introduction

In capillary electrophoresis (CE) and electrochromatography (CEC), an electroosmotic flow (EOF) is used as a driving force. Therefore, CE and CEC come to be an elution type chromatography by applying an electric field [1]. In micro trace analysis (μTAS), EOF is used for the injection of samples, mixing of solutions and developing samples [2], [3].

As to μTAS, EOF was used for the electrokinetic mixing of two reagents at a tee-intersection [2], and for generating a localized pressure flow by using a tee channel [3]. Stroock et al. [4] investigated a technique to generate patterning EOF (e.g., a multidirectional flow and a recirculating cellular flow) in several channels with special surface modifications. Phenomena of electroosmosis on which these studies based are not still understood physically. Further understanding of these phenomena would promote the development of CE, CEC and μTAS.

Electric fields that affect EOF are classified into those perpendicular or parallel to the solid-liquid interface. As for the perpendicular electric field, several studies have been reported so far [5]-[8]. Ghowski et al. [5] calculated the variation of zeta potential in CE with a perpendicular electric field (in the case of capillary, it becomes to be a radial electric field). Chen et al. [6] and Kasicka et al. [7] studied theoretically and experimentally ways to control electroosmosis using a radial electric field in CE. Hayes [8] extended the efficacy of controlling electroosmosis by a radial electric field up to a high pH buffer.

Control of electroosmosis by a perpendicular electric field (a radial field in capillary) has been investigated in detail, while the effect of an electric field parallel to the interface and the EOF direction is still an open question. This is because the Helmholtz-Smoluchowski equation, which is a basic equation of electroosmosis, states that electroosmotic mobility is proportional to a parallel electric field. However, some experimental results were not consistent with the equation.

Terabe et al. [9] and Tsuda [10] studied the relationship between electroosmotic flow velocity (EOFV) and the applied paral-

lel electric field, and found that EOFV was not proportional to the electric field. They also reported that the rate of EOFV rose with increase in the electric field. Chaiyasut et al. [11] reported that EOFV was proportional to an electric field when the field was positive, but not when negative. The reasons for the disagreement between these results and the Helmholtz-Smoluchowski equation have not been found. More adequate data on the relationship between electroosmosis and a parallel electric field are very much awaited.

In this paper, electroosmosis generated by an electric field parallel to the interface was studied using a precisely manufactured apparatus. A donut rather than a capillary channel constructed by a gap between two parallel donut-shaped glass plates was used in the experiment. By applying an electric voltage between the inner and outer sides of the channel, a radial EOF that proceeds from the inner side to the outer side is observed in the channel. It is easy to measure the rate of EOF in a donut channel because the cross-sectional area of the donut channel is considerably larger than that of a usual capillary. Also, the cross-sectional area of the donut channel is adjustable. Since there is no sidewall in a donut channel, a flow between infinitely wide plates (two-dimensional channel) or in a rectangular channel with a large aspect ratio can be simulated. Channels between parallel plates and rectangular channels with large aspect ratios are regarded as two-dimensional. These channels are used for the measurement of particle-zeta potential in solutions [12] and in massive separations. A method of massive separation using both a pressure flow and a cross-electric field in parallel plates channels has been developed by Hirokawa et al. [13] but the separation efficiency is not sufficiently high yet. A massive separation using only EOF has yet to be achieved. Theoretical estimations of EOF in channels between parallel plates and rectangular channels with large aspect ratios were studied [12], [14], and the EOF profiles in a rectangular channel were measured by visualization [15]. In most μTAS [2], [3], various combinations of cross, tee and ell channels are fabricated on microchips. Such channels are usually rectangular with relatively large aspect ratios. Therefore, it is important to clarify the character of EOF between two parallel plates. In this study, EOF in a separation field between wide parallel plates was studied to accumulate basic knowledge for application to separations using EOF.

Electric current can be considered as another important variable in the relation between EOF and a parallel electric field. Terabe et al. reported that the viscosity of fluid was decreased by Joule heat and EOFV was increased by it. Tsuda showed that EOFV was proportional not to the electric field but to the electric current density. It is known that in an electroosmosis channel the electric current along the channel is larger than the current estimated from the conductivity of fluid bulk. Osuga et al. [16] studied the temperature distribution by means of infrared observations and showed that the Joule heat at a methyl alcohol-silica interface was higher than that in the methyl alcohol bulk. They reported that the total electric current along the channel was ten times as large as the current that was estimated from the conductivity of fluid bulk. For our investigation of the relation between EOF and a parallel electric field, the electric current along the channel was measured, resulting in new information about the relationship between electroosmosis and the electric current.

2 Basic equations

From the Helmholtz-Smoluchowski equation, the electroosmotic flow velocity (EOFV), υ_{osm}, is given as [17]

$$\upsilon_{osm} = \frac{\varepsilon E \zeta}{\eta}, \tag{1}$$

where ε, E, ζ and η are the dielectric constant of the liquid, the applied electric field, the zeta potential, and the viscosity, respectively. Assuming that no force acts on liquid and that there is a constant uniform velocity υ_{osm} in the bulk region, the electroosmotic flow rate (EOFR), Q_{osm}, is expressed by [17]

$$Q_{osm} = \frac{\varepsilon E \zeta S}{\eta}, \tag{2}$$

where S is the area of the channel cross section. Note that Q_{osm} is proportional to E as long as ζ is kept constant.

For the donut-shaped channel used in the present study as shown in Figure 1, Eq. (2) has to be altered. It is assumed that the flow is incompressible, steady and axis-symmetric. The electric resistance $dw(r)$ of ring-shaped fluid between radial positions r and $r + dr$ is given as

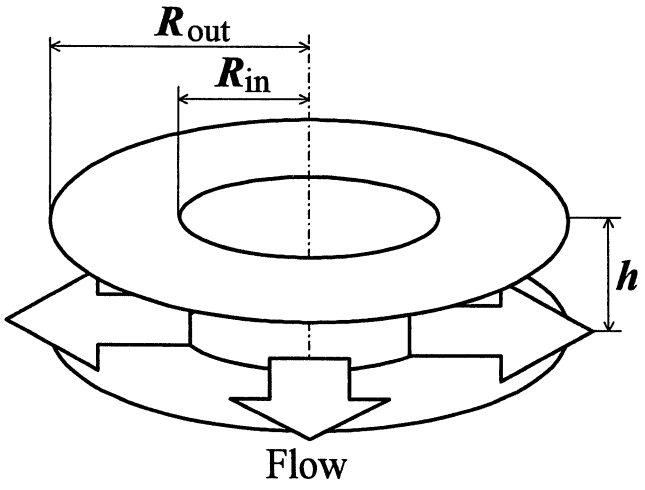

Figure 1. Schematic of the donut channel used in this experiment. Electric fields are radial and electroosmotic flow proceeds radially from inside to outside.

$$dw(r) = \frac{1}{C}\,\frac{dr}{2\pi rh}, \tag{3}$$

where C and h are the electric conductivity of the fluid and the gap between two walls, respectively. The electric voltage $dV(r)$ between r and $r + dr$ is obtained as

$$dV(r) = dw(r)I = \frac{1}{C}\,\frac{dr}{2\pi rh}\,I, \tag{4}$$

where I is the electric current through the donut channel. Therefore, the electric field $E(r)$ is given as:

$$E(r) = \frac{dV}{dr} = \frac{I}{2\pi Chr} \tag{5}$$

Assuming that C is constant, the total electric voltage V is derived as follows:

$$V = \int_{R_{in}}^{R_{out}} E(r)dr = \frac{I}{2\pi Ch}\ln\left(\frac{R_{out}}{R_{in}}\right) \tag{6}$$

Where R_{out} and R_{in} are the outer and inner radii of the channel. Substituting I in Eq. (6) into Eq. (5), we can obtain:

$$E(r) = \frac{V}{r\ln(R_{out}/R_{in})} \tag{7}$$

The Helmholtz-Smoluchowski equation for donut channel is

$$\upsilon_{osm}(r) = \frac{\varepsilon V\zeta}{\eta r\ln(R_{out}/R_{in})}, \tag{8}$$

where $\upsilon_{osm}(r)$ is EOFV. This equation shows that EOFV changes with the radial position. Now assuming zeta potential ζ is constant and the flow velocity is uniform in the wall normal direction, the total flow rate Q_{osm} is expressed as:

$$Q_{osm} = \frac{\varepsilon V\zeta}{\eta}\,\frac{2\pi h}{\ln(R_{out}/R_{in})} \tag{9}$$

In a donut channel, EOFV (υ_{osm}) and the electric field (E) vary in the radial direction. Thus, the applied voltage (V) and EOFR (Q_{osm}) instead of E and υ_{osm} were measured in the present experiment, and EOFV and the electric field at each radial position were estimated from the measured result.

3 Experimental apparatus and methods

3.1 Measurement of electroosmotic flow rate

A schematic diagram of the experimental apparatus used for measurement of EOFR is shown in Figure 2. A gap between two parallel donut-shaped glass plates formed a donut channel. Three pairs of a micrometer head and an electric micrometer were installed to adjust the gap. There were ring-shaped electric terminals that were made of stainless steel (SUS304) inside and outside the channel, and a radial electric field was applied through the channel. Fluid in a buffer tank was passed through a flow meter and was entered the donut channel. The pressure difference ΔP across the inside and outside of the channel was measured using a pressure

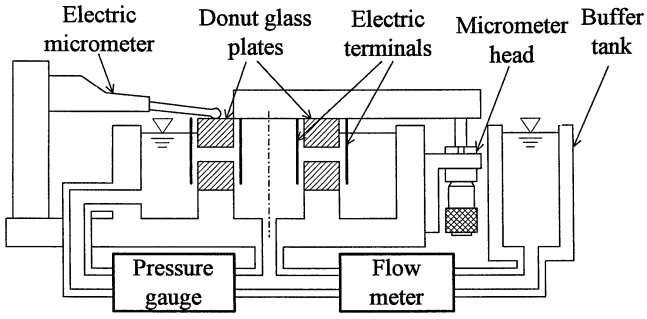

Figure 2. Experimental apparatus.

gauge and was set to zero by adjusting the head of the fluid in the buffer tank. Adjusting the head was done by moving the fluid in and out in the tank through a syringe. The resolution of the pressure gauge was 0.3 [Pa]. The inner diameter, outer diameter and thickness of the donut glass plates were 25, 50 and 10 [mm], respectively. The glass material was BK7 designed for optical purposes, and the flatness error was less than 0.7 [μm] (Sigma Koki Co., Iruma, Saitama). For measurements under simple conditions without the influence of other ions, pure water was used as the working fluid and supplied by a pure water system G-5C (Organo Co., Tokyo). Since the electric conductivity of the water increased with time because water may absorb some gases from the atmosphere (e.g., CO_2), EOFR was measured at the time the conductivity reached a prescribed value. The conductivity was assumed constant within ±0.2 [μS/cm] during measurements because the variation in the conductivity was slow. Thermistor sensors were installed at the inner and outer edges of the channel for measuring the water temperature. The flow rate was measured by a specially designed micro-flow meter [18] within an accuracy of 3% in the range of 0.1 to 2 [mm^3/sec].

3.2 Gap between two glass walls

The gap h between two walls was evaluated using the relation between the Poiseuille flow rate Q_{poi} and the pressure difference ΔP across the inside and outside of the channel. When there is a radial pressure gradient dP/dr in a donut channel, the Poiseuille flow develops whose velocity profile $\upsilon_{poi}(z)$ is given as,

$$\upsilon_{poi} = \frac{1}{2\eta}\frac{dp}{dr}(hz\text{-}z^2), \tag{10}$$

where z is a wall normal position. Integrating this equation with respect to z, the pressure flow rate Q_{poi} is derived as follows:

$$Q_{poi} = \int_0^h \upsilon_{osm}\,dz \times 2\pi r = \frac{\pi rh^3}{6\eta}\frac{dp}{dr} \tag{11}$$

Q_{poi} is independent of r and constant since the fluid is assumed to be incompressible. From this equation, the pressure difference ΔP can be estimated as follows:

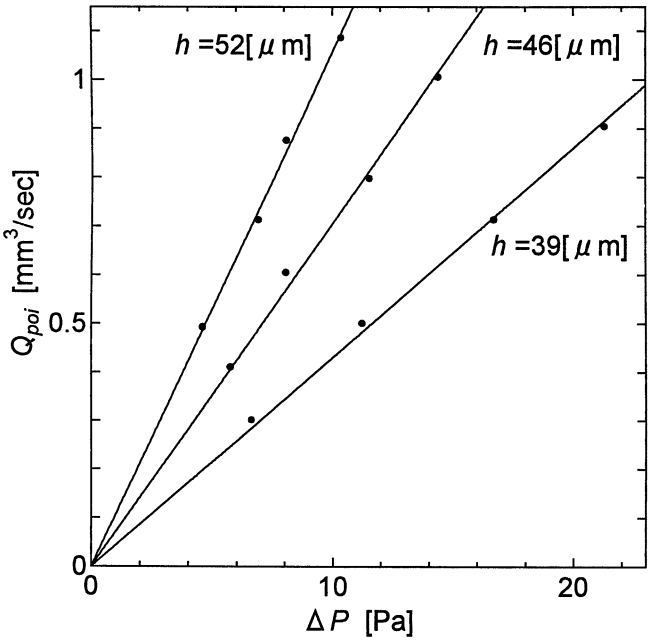

Figure 3. Relationship between the Poiseuille flow rate Q_{poi} and the pressure difference ΔP across the inside and outside of the donut channel. The gaps h calculated from the relation Eq. (4) are 39, 46 and 52 [μm], respectively.

Table 1. Experimental conditions.

No.	C [μS/cm]	h [μm]
1	1	39
2	1	46
3	2	45
4	2	52

$$\int_{R_{in}}^{R_{out}} \frac{dp}{dr}\,dr = \int_{R_{in}}^{R_{out}} \frac{6\,\eta}{\pi r h^3}\,Q_{poi}\,dr$$

$$\Delta P = \frac{6\,\eta \ln\left(R_{out}/R_{in}\right)}{\pi h^3}\,Q_{poi} \qquad (12)$$

So, h is expressed as:

$$h = \sqrt[3]{\frac{6\,\eta \ln\left(R_{out}/R_{in}\right)}{\pi}\,\frac{Q_{poi}}{\Delta P}}, \qquad (13)$$

Figure 3 shows examples of the Q_{poi}-ΔP relation. From the slope of a Q_{poi}-ΔP curve, the gap h can be evaluated by Eq. (13).

3.3 Experimental conditions

The measurements were made under four conditions, i.e., the combinations of two kinds of water conductivity and three gap sizes between the walls (see Table 1).

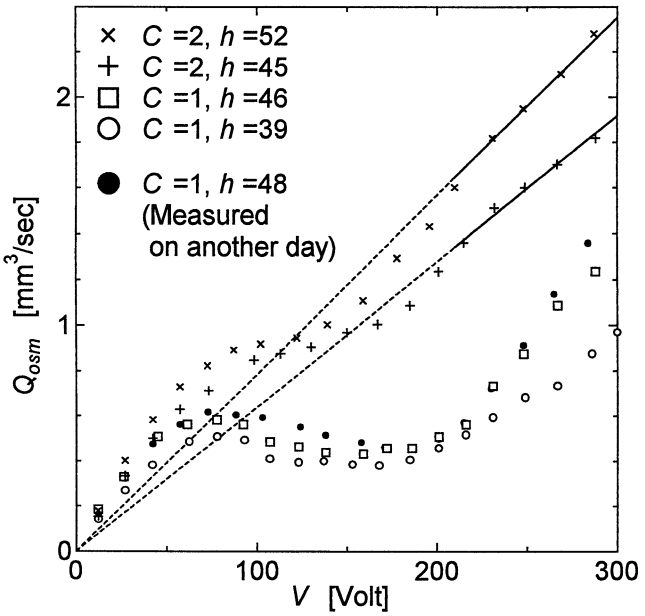

Figure 4. Relationship between the electroosmotic flow rate Q_{osm} and the applied voltage V. The results were obtained under the following conditions: conductivity of water C = 1 [μS/cm] with wall gap h = 39, 46 [μm] and C = 2 [μS/cm] with h = 45, 52 [μm].

4 Results and discussion

4.1 Electroosmotic flow rate

Figure 4 depicts how the experimental results of EOFR Q_{osm} changed against the applied voltage V. The reproducibility of the experiments was checked by comparing experimental results measured on different days under the same condition. The two kinds of data obtained on different days (see (□) and (●) plotted in Figure 4) agreed quite well with each other. So the reproducibility of the experiments was confirmed. Q_{osm} did not show a simple linear relation with V but some wavy variation. This wavy curve of Q_{osm} could be divided into three voltage regions, i.e., $0 \le V \le 50$ [Volt], $50 \le V \le 160$ [Volt] and $160 \le V \le 300$ [Volt]. In the range of $0 \le V \le 50$ [Volt], Q_{osm} increased almost linearly with V. To study the effect of the conductivity C of water on Q_{osm} in this range, we compared those results having the same h but a different C (see (□) and (+) plotted in Figure 5). Both results coincided with each other, and it was found that there was no appreciable effect of C on Q_{osm} in this voltage range. In the range of $50 \le V \le 160$ [Volt], the gradient of the variation curve ($=\partial Q_{osm}/\partial V$) diminished with V. This reduction rate was greater in the case of C = 1 [μS/cm] than for C = 2 [μS/cm]. In case of C = 1 [μS/cm], the gradient became negative in the range of $80 \le V \le 160$ [Volt]; that was Q_{osm} decreased as V increased. Such an effect of C caused quite a large difference in Q_{osm} between C = 1 [μS/cm] and 2 [μS/cm], i.e., Q_{osm} for C = 2 [μS/cm] was twice as large as that for 1

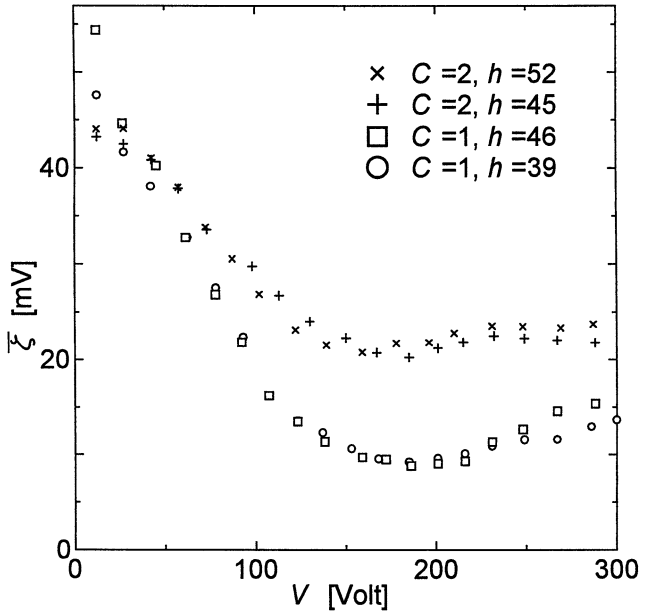

Figure 5. Relationship between the zeta potential $\bar{\zeta}$ and the applied voltage V. $\bar{\zeta}$ was evaluated by substituting Q_{osm} and V into Eq. (9).

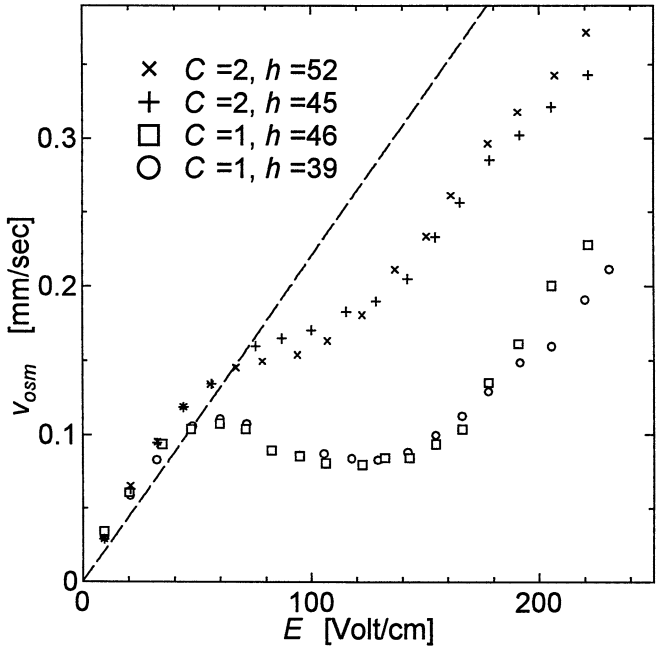

Figure 6. Relationship between the electroosmotic flow velocity and the applied electric field midway between the inner and outer edges of the donut channel. Dashed line shows the electroosmotic mobility given by Dobos

[μS/cm] at V = 160 [Volt]. As V increased beyond 160 [Volt], $\partial Q_{osm}/\partial V$ increased, and Q_{osm} was proportional to V again in the range of $V \geq$ 220 [Volt] for C = 2 [μS/cm]. For C = 1 [μS/cm], however, Q_{osm} was not proportional to V in the range of $160 \leq V \leq$ 300 [Volt].

As described in § 2, the theoretical relation, Eq. (9), gives a linear relation between Q_{osm} and V if ζ is assumed constant. Contrary to the theoretical relation (the Helmholtz-Smoluchowski equation), the present results indicated that a nonlinear relation existed in certain voltage ranges. There are other reports that EOFV is not proportional to the applied voltage. Tsuda [10] reported that the relationship between EOFV and the applied voltage was not linear, and that the increase in the rate of EOFV with the voltage became larger as the voltage increased. In this regard, Terabe et al. [9] explained that it was due to the decrease in liquid-viscosity from the Joule heating effect. In our experiment, we measured the temperature difference of water between the entrance and the exit of the channel and confirmed that the difference was less than 0.5 [℃]. Hence, the effect of Joule heating on EOFR was negligible in our experiments. Therefore, we have to consider the possibility that the zeta potential varied with applied electric fields to explain the nonlinear relation between Q_{osm} and V.

The zeta potential $\bar{\zeta}$ obtained by substituting Q_{osm} and V into Eq. (9) is shown in Figure 5 against V. When Eq. (9) was derived, zeta potential was assumed to be constant. If this assumption was correct, $\bar{\zeta}$ was independent of V and constant. $\bar{\zeta}$, however, varied with V, so the assumption was not correct. Thus, zeta potential depends on the electric field. Since the electric field E varied with the radial position, ζ also varied with the radial position and $\bar{\zeta}$ was the apparent value. The general trend was that $\bar{\zeta}$ decreased with V from ζ_0 (the zeta potential at V = 0 [Volt]) and finally approached some asymptotic values. ζ_0 was around 43 to 55 [mV], and this value was considered to be true ζ but not apparent $\bar{\zeta}$ because E was zero in the whole radial position when V was zero. In the voltage range of $\bar{\zeta}$ was constant, the assumption of constant zeta potential was fullfilled. So $\bar{\zeta}$ derived from Eq. (9) gives true ζ in this range. Therefore, in the case of $V \geq$ 200 [Volt] and C = 2 [μS/cm], the zeta potential is 25 [mV]. It should be noted that the variation in $\bar{\zeta}$ with V was largely affected by the conductivity C. A larger C gave higher $\bar{\zeta}$ except for a small V region ($V \leq$ 50 [Volt]) where no appreciable effect of C existed. In the case of an electrolyte solution, it is known that the zeta potential decreases with an increase in the electrolyte concentration [19]. In the present experiment, however, the zeta potential increased with an increase in conductivity (the densities of ions were assumed to increase). This inconsistency may be due to the rather low densities of ions in water compared to conventional electrolyte solutions.

In Figure 6, the estimated values of EOFV (υ_{osm}) and the electric field (E) midway between the inner and outer edges of the donut channel are shown. The dashed line in the figure shows the electroosmotic mobility of a silica-water interface according to Dobos [20]. The present results clustered around the dashed line of

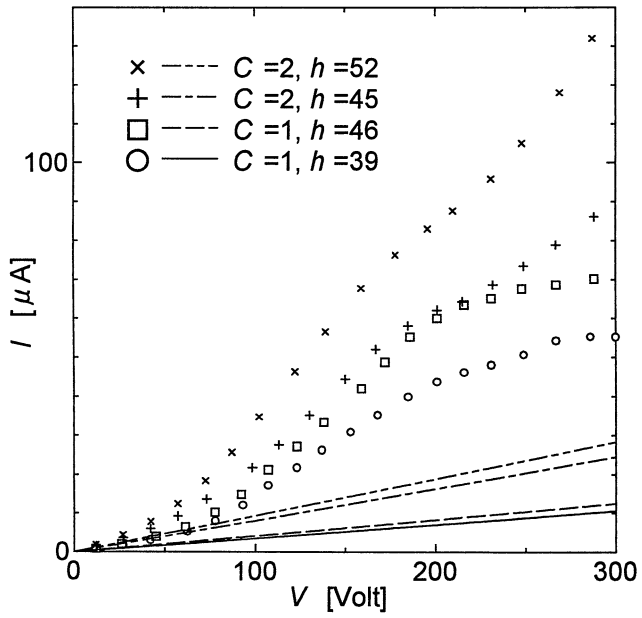

Figure 7. Relationship between the electric current I in the electroosmotic flow channel and the applied voltage V. Lines show the conductive current I_c calculated by Ohm's law using the measured conductivity C of water.

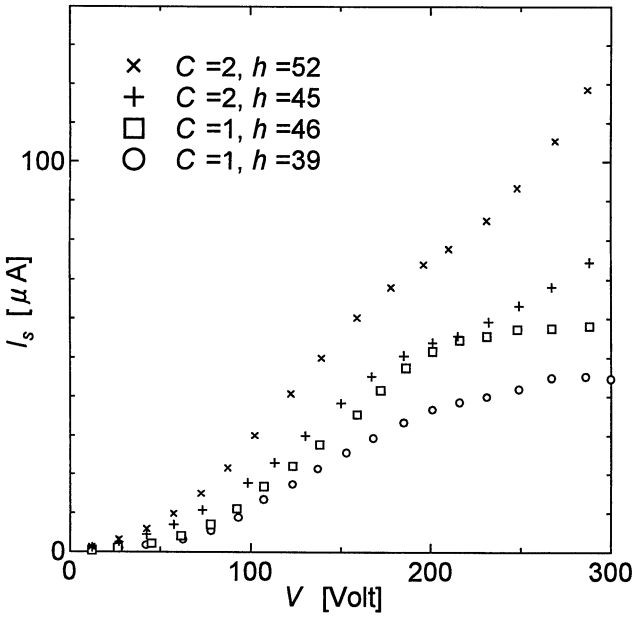

Figure 8. Interface current I_s obtained by substituting measured current I and conductive current I_c into Eq. (14).

Dobos in the range of $0 \leq E \leq 50$ [Volt/cm], but deviated from the dashed line in the range of $E \geq 50$ [Volt/cm].

It is not yet known how an applied parallel electric field affects electroosmotic velocity and/or zeta potential. Chaiyasut et al. [21] observed that the electric resistance of the packed column for CEC varied with the applied voltage, and the relation between the electric resistance and the voltage depended on the charges on the surface. So one reason for zeta potential change can be considered to be that the concentration of the charges in the electric double layer varies with the applied voltage.

4.2 Electric current in electroosmotic flow channel

Figure 7 shows the relationship between the measured electric current I in the donut channel and the applied voltage V. The lines in the figure indicate conductive currents I_c through the bulk calculated by Ohm's law using the measured conductivity C of water. The measured electric current was 2 to 7 times the conductive current of pure water. Comparing two cases, i.e., nearly the same h but different C (see (□) and (+) plotted in Figure 7), the measured currents were almost the same in the range of $V \leq 220$ [Volt] although the conductive current of the latter was twice that of the former. This shows that the electric current in EOF channel is controlled not by the conductive current but by another current.

Here we introduce an additional surface current I_s that passes through the areas near the surfaces of the glass walls. So the measured total current I can be expressed as:

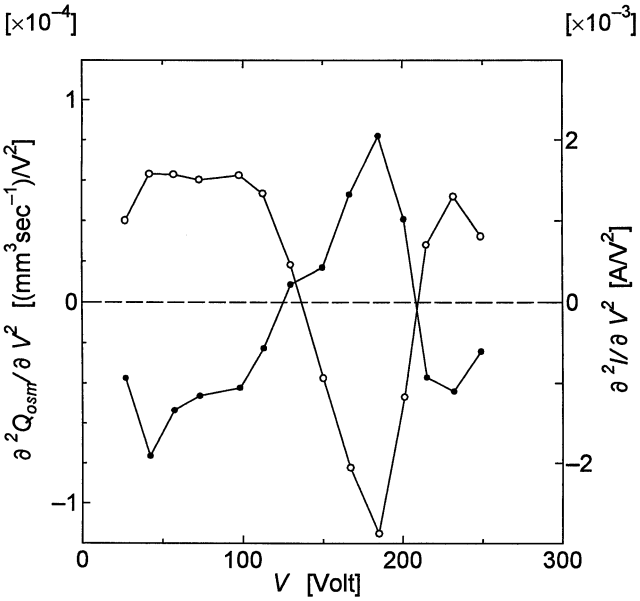

Figure 9. The second-order differentials of Q_{osm} and I against V are compared in the case of C = 2 [μS/cm] and h = 45 [μm]. (●) $\partial^2 Q_{osm}/\partial V^2$, (○) $\partial^2 I/\partial V^2$.

$$I = I_c + I_s \tag{14}$$

I_s, obtained by substituting I and I_c into Eq. (14), is shown in Figure 8. Since I_s is a surface current, it depends only on the conditions in the areas near the surfaces but not on h. Figure 8, however, indicates I_s changed with h. Therefore measured current can not be expressed as the sum of the conductive current and the surface current. This indicates that the current through the bulk would be a

sum of the conductive current and some unknown additional current.

For easy comparison of I and Q_{osm} wavy variations against V, the second-order differentials of Q_{osm} and I ($\partial^2 Q_{osm}/\partial V^2$, $\partial^2 I/\partial V^2$) against V are compared in Figure 9, showing that $\partial^2 Q_{osm}/\partial V^2$ was negative in the voltage range of $\partial^2 I/\partial V^2$ was positive, and vice versa. Thus, there are some relationships between variations in the electroosmosis and the electric current with an applied electric field. These relationships may be one of the causes for the non-linear Q_{osm} -V relation.

5 Concluding remarks

From the experimental results of an electroosmotic flow (EOF) of pure water generated between two glass walls, the following conclusions are obtained. There are electric field ranges in which the electroosmotic flow rate (EOFR) is not proportional to the electric field because the zeta potential varies with the electric field, decreasing for weak electric fields, then increasing for intermediate electric fields, and approaching constant for intensive electric fields. EOFR and zeta potential are largely affected by the conductivity of water. The electric current in an EOF channel is larger than the conductive current and is not proportional to the applied voltage.

Acknowledgements

We would like to express our appreciation to Electro-Mechanic Technology Advancing Foundation for its financial support.

References

[1] Tsuda, T.; Kitagawa, S. *Electric Field Applications in Chromatography, Industrial and Chemical Processes*; Tsuda, T., Ed.; VCH Verlagsgesellschaft mbH, Weinheim and VCH Publishers, Inc., New York. **1995**; Chapter 2.

[2] Jacobson, S. C.; McKnight, T. E.; Ramsey, J. M. *Anal. Chem.* **1999**, *71*, 4455-4459.

[3] Culbertson, C. T.; Ramsey, R. S.; Ramsey, J. M. *Anal. Chem.* **2000**, *72*, 2285-2291.

[4] Stroock, A. D.; Weck, M.; Chiu, D. T.; Huck, W. T. S.; Kenis, P. J. A.; Ismagilov, R. F.; Whitesides, G. M. *Phys. Rev. Lett.* **2000**, *84*, 3314-3317.

[5] Ghowski, K.; Gale, R. J. *J. Chromatogr.* **1991**, *559*, 95-101.

[6] Chen, Y.; Zhu, Y. *Electrophor.* **1999**, *20*, 1817-1821.

[7] Kasivcka, V.; Prusík, Z.; Sázelová, P.; Brynda, E.; Stejskal, J. *Electrophor.* **1999**, *20*, 2484-2492.

[8] Hayes, M. A. *Anal. Chem.* **1999**, *71*, 3793-3798.

[9] Terabe, S.; Otsuka, K.; Ando, T. *Anal. Chem.* **1985**, *57*, 834 -841.

[10] Tsuda, T. *J. Chem. Soc. of Japan* **1986**, *7*, 937-942.

[11] Chaiyasut, C.; Tsuda, T.; Kitagawa, S.; Wada, H.; Monde, T.; Nakabeya, Y. *J. Microcol. Sep.* **1999**, *11*, 590-595.

[12] Fukui, Y.; Yuu, S.; Ushiki, K. *Powder Technol.* **1988**, *54*, 165-174.

[13] Hirokawa, T.; Ikuta, N. *Space Utilization Research* **1999**, *15*, 169-171.

[14] Söderman, O.; Jönsson, B. *J. Chem. Phys.* **1996**, *105*, 10300 -10311.

[15] Tsuda, T.; Ikedo, M.; Jones, G.; Dadoo, R.; Zare, R. N. *J. Chromatogr.* **1993**, *632*, 201-207.

[16] Osuga, T.; Kitagawa, S.; Sakamoto, H.; Tsuda, T. *Jpn. J. Appl. Phys.* **2000**, *39*, 4143-4147.

[17] Tsuda, T. In *Handbook of Capillary Electrophoresis*; Landers, J. P., Ed.; CRC Press, Boca Raton, **1994**; pp. 564-590.

[18] Fujiwara, T.; Kitoh, O. *Trans. Japan Soc. of Mech. Eng. Ser. C* **2001**, *67*, 80-86.

[19] Tsuda, T. *J. Liq. Chromatogr.* **1989**, *12*, 2501-2514.

[20] Dobos, D. *Electrochemical Data*; Akademiai Kiado, Budapest, **1975**; pp. 323.

[21] Chaiyasut, C.; Kitagawa, S.; Wada H.; Tsuda, T. *Anal. Sci.* **2000**, *16*, 413-416.